Dimensional reduction applied to an intelligent model for boost converter switching operation

Luis-Alfonso Fernandez-Serantes[1], José-Luis Casteleiro-Roca[1], Paulo Novais[2], Dragan Simić[3], and José Luis Calvo-Rolle[1]

Abstract The dimensional reduction algorithms are applied to a hybrid intelligent model that distinguishes the switching operating mode of a boost converter. Thus, the boost converter has been analyzed and both operating mode are explained, distinguishing between Hard-switching and Soft-switching modes. Then, the dataset is created out of the data obtained from simulation of the real circuit and the hybrid intelligent classification model is implemented. Finally, the dimensional reduction of the input variables is carried out and the results are compared. As result, the proposed model with the applied dimensional reduced dataset is able to distinguish between the HS and SS operating modes with high accuracy.

Key words: Hard-switching, soft-switching, boost converter, power electronics, classification, dimensional reduction

1 Introduction

Nowadays, multiple research approaches are applied in the power electronics field, where the focus is kept on increasing the efficiency of the power converter; thus, reducing the size and weight of the circuits. The recent studies centre the attention on the use of the wide band-gap (WBG) materials such as Silicon Carbide (SiC) and Gallium Nitride (GaN) and the use of soft-switching techniques [1, 4]. The introduction of SiC and GaN materials in the power converters initiated replacement of the silicon as manufacturing material of the power transistors [23, 8]. They are

University of A Coruña, CTC, CITIC,
Department of Industrial Engineering, Ferrol, A Coruña, Spain
, e-mail: luis.alfonso.fernandez.serantes@udc.es · University of Minho, Algoritmi Center
Department of Informatics, Braga, Portugal · University of Novi Sad,
Faculty of Technical Sciences,
Trg Dositeja Obradovića 6, 21000, Novi Sad, Serbia

more competitive, provide better performance and characteristics in comparison with silicon transistors, such as higher switching speeds, higher breakdown voltages, lower on-state resistance, etc. Additionally, in the last years the production prices have reduced, making them more interesting for the industry [8, 17, 15].

In order to improve the efficiency of the existing converters, the soft- switching techniques are widely introduced. These techniques allow a reduction of the switching losses during the converter operation. Moreover, the new materials, SiC and GaN, make more interesting these techniques in addition to their intrinsic characteristics [23, 9].

Along with the introduction of the Artificial Intelligence (AI) in other fields, the AI starts gaining also importance in the power electronics. These techniques are used for supporting the development and design processes, as described in [26, 2] where the AI are used to design magnetic components. Or, another application, to improve the performance of the power converters with the development of new control schemes, as done in [25, 14, 12].

With the aim of controlling and maintaining the converter operating in soft-switching and, therefore, delivering the maximum efficiency, the classification of the operating mode needs to be realized. When the converter operates in SS mode in comparison with HS mode, the switching losses are reduced. Thus, assuring that the converter operates in the desired mode becomes of importance.

In this work, the proposed method to detect the operating mode is based on AI. By measuring different signals of the converter, the AI is able to detect the operating mode, helping the designer to optimize the converter by reducing the switching losses and increasing the transfer of energy.

A dimensional reduction of the dataset used by the model is presented. This reduction of data helps to increase the speed and reduce computational cost of classifier, and further improve the performance of the model to detect the operating mode of the power converter.

The paper is structured as follows: first, an analysis of a synchronous rectified boost converter is explained in section 2. The applied dimensional reduction to the proposed model is described in the next section, 3, along with the generated dataset and classification techniques. Then, the performance and efficiency of the proposed model with the different dimensional reduction methods is presented in section 4 and finally, conclusions are drawn in section 5.

2 Case Study

The analysis of a synchronous rectified boost converter is done in this section. The converter topology is shown in the figure 1. The components used in this converter are two transistors, high-side and low-side transistors, which operate in a complementary manner. The transistors generate a pulsed voltage that varies from input voltage and ground, at the switching node (Vsw), which is then filtered. An input capacitor is used to filter the peak currents drawn by the converter. The output filter is made up

of an inductor and a capacitor, which filters the pulse voltage of the switching node obtaining a constant output voltage.

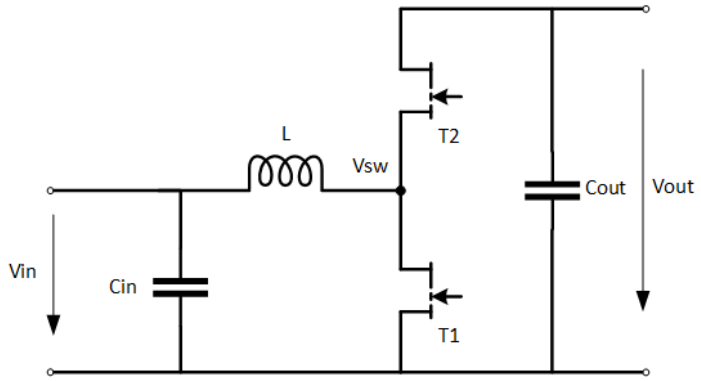

Fig. 1 Synchronous rectified boost converter.

Traditionally, the described converter operates in Hard-Switching (HS) mode: meaning that losses occur during the switching transitions due to the current and voltage at the transistor during commutation. When the transistor is turned-off, the voltage is blocked and no current is flowing. When a signal is applied to the transistor's gate and the commutation starts, the resistance of the channel starts to drop as the current starts flowing through the transistor. During this time, the voltage drops while the current rises, occurring switching losses as $P = V \cdot I$. In HS mode, this process happens during turn-on and turn-off commutation. Moreover, when the transistor is switched on, the losses are caused by the on-state resistance times the flowing current: $P_{conduction} = I^2 \cdot R_{on-state}$.

In addition to the losses caused by the concurrent of current and voltage, the parasitic capacitance of the transistor (Coss) is reloaded and discharged through the transistor channel, causing further switching losses. These losses can be calculated as $P = \frac{1}{2} \cdot C_{oss} \cdot V^2$.

In the figure 2, the converter losses in HS mode are represented, where the switching losses can be seen.

Intending to improve the efficiency of the synchronous rectified boost converter, the other operating mode is introduced: soft-switching (SS) mode. In this case, either the current or the voltage through the transistor channels is brought to zero. If the current is zero at the switching instant, it is called Zero-Current-Switching (ZCS); on the other hand, if the voltage across the transistor at the switching instant is zero, the SS mode is due to Zero-Voltage-Switching (ZVS).

When the converter operates in SS, the losses during the commutation are nearly zero, as either the voltage or current are zero: $P = V \cdot I = 0 \cdot I$ or $P = V \cdot 0$. The figure 2, shows the transitions in the SS operating mode.

The conditions of SS are achieved thanks to the resonance between the components of the circuit, such as a resonance LC tank. Moreover, in the proposed

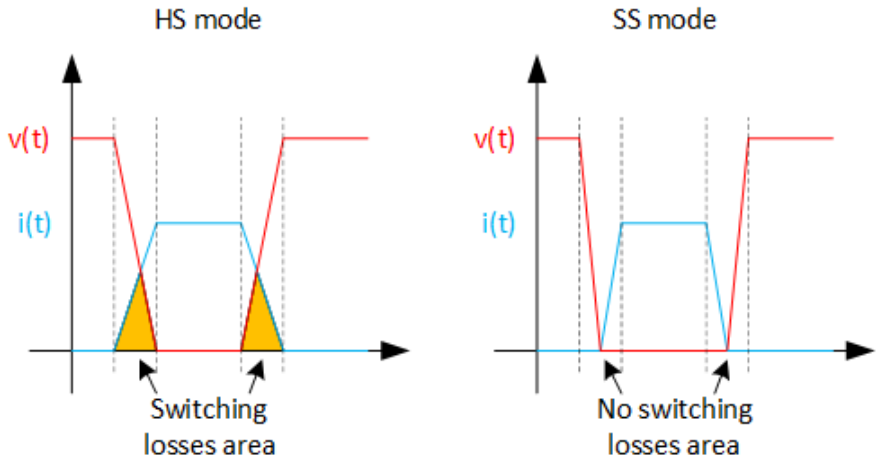

Fig. 2 Hard- and Soft-switching transitions with different current ripple.

converter, the resonance happens between the filter inductor and the parasitic output capacitance of the transistor (Coss), using this capacitance as a non-dissipative snubber [22, 3].

In the synchronous rectified boost converter, the used method for the SS operation is the ZVS and it is achieved during turn-on of the high-side switch.

In the ZVS method, the switches turn-on or -off when the voltage across the transistor is zero. Thus, when the high-side transistor switches off, the current moves to the low-side switch. During the interlock delay, time where both switches are off, the current flows through the antiparallel diode of the low-side transistor, equalizing the voltage across this transistor, causing a ZVS switching of the low-side transistor.

During the time that the low-side transistor is on, the current starts decreasing in the inductor until the current reaches a negative value, flowing from the load to the switches. At this instant, when the current is negative, the low-side switch turns-off. The current at the inductor does not have a path to flow, so it will charge the output capacitance of the transistors, rising the voltage at the switching node.

Once the voltage at the switching node reaches the input voltage, the antiparallel of the high-side switch starts conducting, instant when this switch can turn-on with ZVS.

At this point, the high-side transistor can switch lossless, as the voltage across is just a few volts from the forward diode voltage [22, 19].

When using this topology in SS mode, the design of the inductor is very important, as it needs to allow high ripple current..

Traditionally, the designer and developers keep the inductor ripple low, between 10% and 30% of the output current. The definition of the inductance value is done according to the equation 1, where the inductor value depends on the switching frequency, output voltage and the allowed current ripple.

$$L = \frac{V_{in} \cdot (V_{out} - V_{in})}{f \cdot I_{ripple} \cdot V_{out}} \tag{1}$$

where L is the inductance value of the inductor, V_{in} is the input voltage to the circuit, V_{out} is the output voltage from the converter, f is the switching frequency and I_{ripple} is the current ripple in the inductor.

With the introduction of this converter operating in SS mode, the design of the inductor needs to be reconsidered. In this mode, the ripple of the current allows the current to drop to zero and beyond, defining the Triangular Current Mode (TCM) [5, 13, 7].

As mentioned above, when the current ripple is kept low, as shown in the figure 3, the converter operates in HS mode, as the ZVS condition is never reached. In opposition, when the current ripple allows the current to drop below zero, the switching losses in the converter can be reduced due to the ZVS mode.

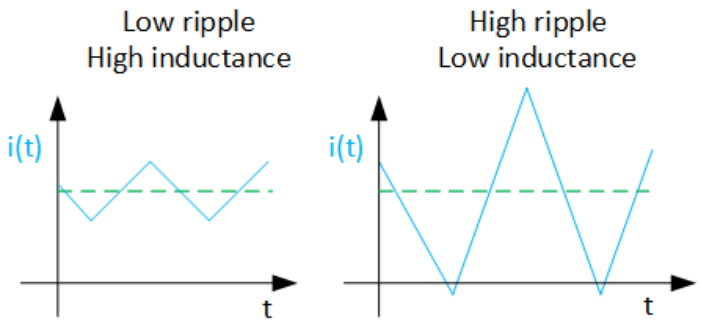

Fig. 3 Current ripple with different filter inductors.

The SS operating mode allows a reduction of the switching losses but with the drawback of increasing the conduction losses, as the Root Means Square (RMS) of the current increases. In order to take advantage of this operating mode, the switching frequency of the converter is increased, reducing in this manner the conduction losses and the filter components; therefore further increasing the power densities of the converter.

3 Model Approach

In this research, a dimensional reduction of the data used by the classification model has been done. The classification model aims to detect and distinguish the operating mode of the converter, between HS and SS mode. Three different dimensional

reduction techniques are applied with the aim of reducing the computational cost of the classifier and improving the performance and efficiency.

In the figure 4, the steps followed to build the classification model are shown. First, the simulation data is obtained and pre-processed to obtain more significant parameters which provide detail information about the converter operating mode. Then, the reduction of the data is applied and finally the classification algorithms are used to determine if the converter is in either HS or SS mode.

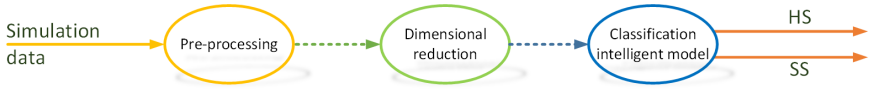

Fig. 4 Model approach.

3.1 Dataset

The dataset used in this work is obtained from simulation results of the synchronous rectified boost converter by using the LTSpice simulation software. With the aim of obtaining closer results to the real circuit, the transistors models from the manufacturer have been used.

Up to 80 simulations have been done with the proposed circuit of the figure 1. The converter is operated in both HS and SS modes. To allow reproducibility of the experiments and results, the converter keeps unchanged and just the applied load is varied. The complete dataset is compound of 50% of HS data and the other 50% of SS data.

The dataset is made up from the following signals measured in the circuit:

- Input voltage: a constant input voltage of 200 V is applied to the circuit.
- Output voltage: the output voltage of the converter is kept at 400 V, allowing a ripple from 390 V up to 410 V.
- Switching node voltage (Vsw node figure 1): at this node, the voltage varies from 0 V when the low-side switch is on up to 400 V when the high-side switch is on. The generated signal is square with a frequency varying from 80 kHz up to 2 MHz.
- Inductor current: is a triangular waveform. The average current depends on the output load and the current ripple depends on the switching frequency. For a constant inductance value, when the switching frequency is higher, the current ripple is lower, while it increases as the switching frequency decreases. In HS mode, the ripple is between 10 % to 30 % while in SS mode, the ripple increases above 200 %.
- Output current: is constant, filtered by the inductor and capacitor, and its value depends on the connected load to the converter.

Then, from this initial dataset, a pre-processing is done for the purpose of obtaining more significant measurements: the base for this pre-processing is the raw data of the switching node voltage (Vsw); then, the first and second derivative are calculated, removing the on- and off-states while keeping the information of the commutations.

Furthermore, the rising and falling edges of the Vsw are isolated, as shown in the figure 5. This allows to focus the model on the transitions, which provides details of the operating mode, either HS or SS mode. The rising and falling times are also obtained (*tr* and *tf*).

Moreover, the first and second derivatives are also applied to the rising and falling edge signal explained above. Additionally, the integral of the edges is calculated.

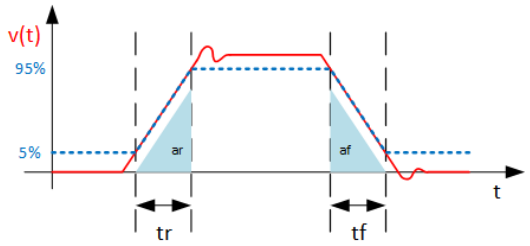

Fig. 5 Rising and falling edge of the switching node voltage, in dashed blue, and the original signal in continuous red.

As described, 8 signals are obtained from the Vsw: the raw data (red signal in figure 5), the first and the second derivatives of the raw data, the rising/falling edge data (dotted blue signal in figure 5), the first and second derivatives of rising/falling edge data, the rising edge integral (area at the rising edge, *ar*, in figure 5) and the falling edge integral (area at the falling edge, *af*, in figure 5).

Moreover, the following statistics and indicators are calculated from the 8 obtained signals: average, standard deviation, variance, co-variance, Root Mean Square and Total Harmonic Distortion (THD). Resulting in a matrix of 8x6 for each of the 80 simulations.

Moreover, previous application of the dimensional reduction algorithms, the data has been parameterized.

3.2 Methods

The dimensional reduction algorithms used in this research are the self-organizing map (SOM), the correlation matrix and the principal component analysis (PCA).

3.2.1 Self-organizing map (SOM)

Self-organizing maps learn to cluster data based on similarity, topology, with a preference of assigning the same number of instances to each class. Self-organizing maps are used both to cluster data and to reduce the dimensionality of data [24].

In SOM method, the dimensional reduction is completed by visualization techniques. The procedure is executing the SOM algorithm and with the obtained map results for each variable and taking into account the similarity, the reduction is accomplished by discarding the less convenient variable.

3.2.2 Correlation matrix

A correlation matrix is a table showing correlation coefficients between variables. Each cell in the table shows the correlation between two variables. A correlation matrix is used to summarize data, as an input into a more advanced analysis, and as a diagnostic for advanced analyses [18].

3.2.3 Principal component analysis (PCA)

Principal component analysis (PCA) is one of the classical dimensionality reduction algorithms, which guarantees the minimum mean square error and gains linearly independent vectors as the basis of subspace [18].

3.3 Classification model

3.3.1 Multilayer Perceptron

A multilayer perceptron is an artificial neural network with multiple hidden layers of neurons. The structure is the following: one input layer, with the input features to the algorithm, then the multiple hidden layer which have neurons with an activation function, and one output layer, which number of neurons depends on the desired outputs. All these layers are connected in between by weighted connections that are tuned with the aim of decreasing the error of the output [25, 11, 7].

3.3.2 Linear Discrimination Analysis

This method projects the data from a high dimensional space into a low-dimensional space. This method uses a weight vector W, which projects the given set of data vector E in such a way that maximizes the class separation of the data but minimizes

the intra-class data [27, 10]. The separation is good when the projections of the class involve exposing long distance along the direction of vector W [21, 6].

3.3.3 Support vector machine

The algorithm tries to find two parallel hyper-planes that maximize the minimum distance between two class of samples [20]. Therefore, the vectors are defined as training instances presented near the hyperplane and the projection of the dataset is done in a high dimensional feature space using a kernel operator [20].

3.3.4 Ensemble

The term ensemble is used to define multiple classification methods which are used in combination with the aim of improving the performance over single classifiers [16]. They are commonly used for classification tasks. The ensemble does a regularization, process of choosing fewer weak learners in order to increase predictive performance [28].

3.4 Experiments description

The experiments carried out aims to show the performance of the classification algorithms and to validate the improvement achieved by the dimensional reduction.

First, the dataset is divided into two different groups. The first group, that contains 75% of the generated data, is used to train the proposed models; while the rest, 25 % of the dataset, is used to validate the proposed algorithms. It is important to remark that the separation is done randomly.

The following algorithms are trained and then validated with the previously mentioned datasets:

- Multilayer perceptron (MLP): uses the Levenberg-Marquardt backpropagation algorithm with an hidden layer with 1 up to 10 neurons.
- Linear discrimination analysis (LDA): the used type is the regularized LDA, where all the classes have identical co-variance matrix.
- Support vector machine (SVM): The linear kernel function has been used. The classifier has been trained using the standardized predictors, which centers and scales each predictor variable by the corresponding mean and standard deviation.
- Ensemble: the adaptive logistic regression has been used. This type is commonly applied to binary classification. The number of cycles has been varied in steps of 10 from 10 up to 100. The weak-learners used function is the decision tree.

Finally, once the different models are trained, the models are validated using the previously separated 25 % of the data. This is done to verify the correct functionality

and performance of the proposed models. The classification results obtained from the models are then compared with the validation data and by using a confusion matrix, the different statistics are calculated.

In a following step, the proposed dimensional reduction methods are applied to the dataset. The different models are used again with this reduced data and the performance is measured. The dimensional reduction methods used are:

- SOM: Train with size of 20 two-dimensional map.
- Correlation matrix: the values close to 1 or -1 indicate that there is a linear relationship between the data columns and they can be removed, leaving the values that are equal or close to 0, that suggest that these data are not related. The chosen limit to differentiate the variables is 0.33.
- PCA: a new matrix is created with different weights of the data. The data in this matrix has no relation with the input data.

4 Results

The table 1 shows the classification performance of the model approach by applying different dimensional reduction methods. When no reduction is used, the best achieved performance was by the MLP7 with 97.06 % of accuracy while when using the dimensional reduction methods, the accuracy increases up to 100% of right classification.

The obtained data reduction by the different applied techniques is the following:

- SOM: a reduction of 33 variables has been achieved, meaning that 70% of the data is removed.
- Correlation matrix: in this case, 37 variables are discarded, reducing the size of the data matrix by 78%.
- PCA: a new matrix of data has been created with different weights of the parameters.

As summary, the performance and accuracy in percentage that each classification technique achieves with the dimensional reduction of the input data is shown in the table 1.

5 Conclusions and future works

In this research different dimensional reduction methods are applied to a classification model used to detect the operating mode of a synchronous rectified boost converter with the aim of increasing the classification accuracy and reducing the computational cost.

The used dataset is obtained from the simulation of the synchronous rectified boost converter and the most significant variables are selected to perform the classification.

Table 1 Summary of the results.

Classification method	Dimensional reduction methods			
	Without reduction	SOM	Corr. Matrix	PCA
MLP1	81.54	89.47	91.89	28.57
MLP2	73.53	94.74	94.59	36.36
MLP3	62.26	94.74	94.59	27.78
MLP4	55.88	100	100	42.10
MLP5	79.41	86.11	94.60	35.00
MLP6	60.29	92.11	92.15	52.94
MLP7	97.06	100	97.30	23.53
MLP8	73.53	92.11	94.59	42.10
MLP9	86.77	97.37	100	38.89
MLP10	52.94	100	97.30	21.74
SVM	77.94	94.74	91.89	39.29
LDA	60.29	86.84	94.59	46.43
Ensemble10	51.47	97.37	89.20	96.43
Ensemble20-100	51.47	94.74	86.48	96.43

In order to compare the performance of the dimensional reduction, three different algorithms have been applied: SOM, correlation matrix and PCA. The achieved dimensional reduction of the data is 70% when using SOM and 78% when using the correlation matrix. In case of using PCA, a new matrix has been built.

The results achieved by the classification models are compared, when no dimensional reduction model is used and when the proposed methods are applied. When SOM algorithm is used, the performance is increase up to 100% with the MLP4, MLP5 and MLP10 classifiers. Moreover, the correlation matrix increases the accuracy of the MLP4 and MLP9 classifiers up to 100%. Although the accuracy with the PCA method applied to the models does not achieve the 100%, the performance of the Ensemble classifiers is increased from 51% up to 96%.

In addition to the increase of the accuracy, the dimensional reduction reduces the input dataset by 70% in case of using SOM and by 78% while using the correlation matrix.

The research in this field will follow by the development of a hybrid intelligent model that aims to further improve the accuracy of the classifiers. Moreover, the real circuit will be implemented and the models will be applied to real measured data from the power converter.

Acknowledgements CITIC, as a Research Center of the University System of Galicia, is funded by Consellería de Educación, Universidade e Formación Profesional of the Xunta de Galicia through the European Regional Development Fund (ERDF) and the Secretaría Xeral de Universidades (Ref. ED431G 2019/01).

References

1. Al-bayati, A.M.S., Alharbi, S.S., Alharbi, S.S., Matin, M.: A comparative design and performance study of a non-isolated dc-dc buck converter based on si-mosfet/si-diode, sic-jfet/sic-schottky diode, and gan-transistor/sic-schottky diode power devices. In: 2017 North American Power Symposium (NAPS), pp. 1–6 (2017). DOI 10.1109/NAPS.2017.8107192
2. Aláiz-Moretón, H., Castejón-Limas, M., Casteleiro-Roca, J.L., Jove, E., Fernández Robles, L., Calvo-Rolle, J.L.: A fault detection system for a geothermal heat exchanger sensor based on intelligent techniques. Sensors **19**(12), 2740 (2019)
3. Casado-Vara, R., Sittón-Candanedo, I., la Prieta, F.D., Rodríguez, S., Calvo-Rolle, J.L., Venayagamoorthy, G.K., Vega, P., Prieto, J.: Edge computing and adaptive fault-tolerant tracking control algorithm for smart buildings: A case study. Cybernetics and Systems **51**(7), 685–697 (2020). DOI 10.1080/01969722.2020.1798643. URL https://doi.org/10.1080/01969722.2020.1798643
4. Casteleiro-Roca, J.L., Javier Barragan, A., Segura, F., Luis Calvo-Rolle, J., Manuel Andujar, J.: Intelligent hybrid system for the prediction of the voltage-current characteristic curve of a hydrogen-based fuel cell. Revista Iberoamericana de Automática e Informática industrial **16**(4), 492–501 (2019)
5. Fernandez-Serantes, L.A., Berger, H., Stocksreiter, W., Weis, G.: Ultra-high frequent switching with gan-hemts using the coss-capacitances as non-dissipative snubbers. In: PCIM Europe 2016; International Exhibition and Conference for Power Electronics, Intelligent Motion, Renewable Energy and Energy Management, pp. 1–8. VDE (2016)
6. Fernandez-Serantes, L.A., Casteleiro-Roca, J.L., Berger, H., Calvo-Rolle, J.L.: Hybrid intelligent system for a synchronous rectifier converter control and soft switching ensurement. Engineering Science and Technology, an International Journal p. 101189 (2022)
7. Fernandez-Serantes, L.A., Casteleiro-Roca, J.L., Calvo-Rolle, J.L.: Hybrid intelligent system for a half-bridge converter control and soft switching ensurement. Revista Iberoamericana de Automática e Informática industrial (2022). DOI https://doi.org/10.4995/riai.2022.16656
8. Fernández-Serantes, L.A., Vázquez, R.E., Casteleiro-Roca, J.L., Calvo-Rolle, J.L., Corchado, E.: Hybrid intelligent model to predict the soc of a lfp power cell type. In: International conference on hybrid artificial intelligence systems, pp. 561–572. Springer (2014)
9. García-Ordás, M.T., Alaiz-Moretón, H., Casteleiro-Roca, J.L., Jove, E., Benítez-Andrades, J.A., García-Rodríguez, I., Quintián, H., Calvo-Rolle, J.L.: Clustering techniques selection for a hybrid regression model: A case study based on a solar thermal system. Cybernetics and Systems **0**(0), 1–20 (2022). DOI 10.1080/01969722.2022.2030006. URL https://doi.org/10.1080/01969722.2022.2030006
10. Gonzalez-Cava, J.M., Arnay, R., Mendez-Perez, J.A., León, A., Martín, M., Reboso, J.A., Jove-Perez, E., Calvo-Rolle, J.L.: Machine learning techniques for computer-based decision systems in the operating theatre: application to analgesia delivery. Logic Journal of the IGPL **29**(2), 236–250 (2020). DOI 10.1093/jigpal/jzaa049. URL https://doi.org/10.1093/jigpal/jzaa049
11. Jove, E., Casteleiro-Roca, J., Quintián, H., Méndez-Pérez, J., Calvo-Rolle, J.: Anomaly detection based on intelligent techniques over a bicomponent production plant used on wind generator blades manufacturing. Revista Iberoamericana de Automática e Informática industrial **17**(1), 84–93 (2020)
12. Jove, E., Casteleiro-Roca, J.L., Casado-Vara, R., Quintián, H., Pérez, J.A.M., Mohamad, M.S., Calvo-Rolle, J.L.: Comparative study of one-class based anomaly detection techniques for a bicomponent mixing machine monitoring. Cybernetics and Systems **51**(7), 649–667 (2020). DOI 10.1080/01969722.2020.1798641. URL https://doi.org/10.1080/01969722.2020.1798641
13. Jove, E., Casteleiro-Roca, J.L., Quintián, H., Méndez-Pérez, J.A., Calvo-Rolle, J.L.: A fault detection system based on unsupervised techniques for industrial control loops. Expert Systems **36**(4), e12395 (2019)
14. Jove, E., Casteleiro-Roca, J.L., Quintián, H., Simić, D., Méndez-Pérez, J.A., Luis Calvo-Rolle, J.: Anomaly detection based on one-class intelligent techniques over a control level plant. Logic Journal of the IGPL **28**(4), 502–518 (2020)

15. Jove, E., Casteleiro-Roca, J.L., Quintián, H., Méndez-Pérez, J.A., Calvo-Rolle, J.L.: A new method for anomaly detection based on non-convex boundaries with random two-dimensional projections. Information Fusion **65**, 50–57 (2021). DOI https://doi.org/10.1016/j.inffus.2020.08.011. URL https://www.sciencedirect.com/science/article/pii/S1566253520303407
16. Jove, E., Gonzalez-Cava, J.M., Casteleiro-Roca, J.L., Méndez-Pérez, J.A., Antonio Reboso-Morales, J., Javier Pérez-Castelo, F., Javier de Cos Juez, F., Luis Calvo-Rolle, J.: Modelling the hypnotic patient response in general anaesthesia using intelligent models. Logic Journal of the IGPL **27**(2), 189–201 (2019)
17. Jove, E., Gonzalez-Cava, J.M., Casteleiro-Roca, J.L., Quintián, H., Méndez Pérez, J.A., Vega Vega, R., Zayas-Gato, F., de Cos Juez, F.J., León, A., MartÍn, M., Reboso, J.A., Wozniak, M., Luis Calvo-Rolle, J.: Hybrid Intelligent Model to Predict the Remifentanil Infusion Rate in Patients Under General Anesthesia. Logic Journal of the IGPL **29**(2), 193–206 (2020). DOI 10.1093/jigpal/jzaa046. URL https://doi.org/10.1093/jigpal/jzaa046
18. Kaski, S., Sinkkonen, J., Klami, A.: Discriminative clustering. Neurocomputing **69**(1-3), 18–41 (2005)
19. Leira, A., Jove, E., Gonzalez-Cava, J.M., Casteleiro-Roca, J.L., Quintián, H., Zayas-Gato, F., Álvarez, S.T., Simic, S., Méndez-Pérez, J.A., Luis Calvo-Rolle, J.: One-Class-Based Intelligent Classifier for Detecting Anomalous Situations During the Anesthetic Process. Logic Journal of the IGPL (2020). DOI 10.1093/jigpal/jzaa065. URL https://doi.org/10.1093/jigpal/jzaa065. Jzaa065
20. Liu, M.Z., Shao, Y.H., Li, C.N., Chen, W.J.: Smooth pinball loss nonparallel support vector machine for robust classification. Applied Soft Computing p. 106840 (2020). DOI 10.1016/j.asoc.2020.106840
21. Marchesan, G., Muraro, M., Cardoso, G., Mariotto, L., da Silva, C.: Method for distributed generation anti-islanding protection based on singular value decomposition and linear discrimination analysis. Electric Power Systems Research **130**, 124 – 131 (2016). DOI 10.1016/j.epsr.2015.08.025
22. Mohan, N., Undeland, T.M., Robbins, W.P.: Power electronics: converters, applications, and design. John wiley & sons (2003)
23. Neumayr, D., Bortis, D., Kolar, J.W.: The essence of the little box challenge-part a: Key design challenges solutions. CPSS Transactions on Power Electronics and Applications **5**(2), 158–179 (2020). DOI 10.24295/CPSSTPEA.2020.00014
24. Qin, A.K., Suganthan, P.N.: Enhanced neural gas network for prototype-based clustering. Pattern recognition **38**(8), 1275–1288 (2005)
25. Tahiliani, S., Sreeni, S., Moorthy, C.B.: A multilayer perceptron approach to track maximum power in wind power generation systems. In: TENCON 2019 - 2019 IEEE Region 10 Conference (TENCON), pp. 587–591 (2019). DOI 10.1109/TENCON.2019.8929414
26. Tao Liu, Wenjun Zhang, Zhiping Yu: Modeling of spiral inductors using artificial neural network. In: Proceedings. 2005 IEEE International Joint Conference on Neural Networks, 2005., vol. 4, pp. 2353–2358 vol. 4 (2005). DOI 10.1109/IJCNN.2005.1556269
27. Thapngam, T., Yu, S., Zhou, W.: Ddos discrimination by linear discriminant analysis (lda). In: 2012 International Conference on Computing, Networking and Communications (ICNC), pp. 532–536. IEEE (2012)
28. UYSAL, I., GÖVENIR, H.A.: An overview of regression techniques for knowledge discovery. The Knowledge Engineering Review **14**, 319–340 (1999)